The Nucleolin Targeting Aptamer AS1411 Destabilizes *Bcl-2* Messenger RNA in Human Breast Cancer Cells

Sridharan Soundararajan,[1] Weiwei Chen,[1] Eleanor K. Spicer,[1] Nigel Courtenay-Luck,[2] and Daniel J. Fernandes[1]

[1]Department of Biochemistry and Molecular Biology, Medical University of South Carolina, Charleston, South Carolina and [2]Antisoma Research, Ltd., London, United Kingdom

Abstract

We sought to determine whether nucleolin, a *bcl-2* mRNA-binding protein, has a role in the regulation of *bcl-2* mRNA stability in MCF-7 and MDA-MB-231 breast cancer cells. Furthermore, we examined the efficacy of the aptamer AS1411 in targeting nucleolin and inducing *bcl-2* mRNA instability and cytotoxicity in these cells. AS1411 at 5 μmol/L inhibited the growth of MCF-7 and MDA-MB-231 cells, whereas 20 μmol/L AS1411 had no effect on the growth rate or viability of normal MCF-10A mammary epithelial cells. This selectivity of AS1411 was related to a greater uptake of AS1411 into the cytoplasm of MCF-7 cells compared with MCF-10A cells and to a 4-fold higher level of cytoplasmic nucleolin in MCF-7 cells. Stable siRNA knockdown of nucleolin in MCF-7 cells reduced nucleolin and bcl-2 protein levels and decreased the half-life of *bcl-2* mRNA from 11 to 5 hours. Similarly, AS1411 (10 μmol/L) decreased the half-life of *bcl-2* mRNA in MCF-7 and MDA-MB-231 cells to 1.0 and 1.2 hours, respectively. In contrast, AS1411 had no effect on the stability of *bcl-2* mRNA in normal MCF-10A cells. AS1411 also inhibited the binding of nucleolin to the instability element AU-rich element 1 of *bcl-2* mRNA in a cell-free system and in MCF-7 cells. Together, the results suggest that AS1411 acts as a molecular decoy by competing with *bcl-2* mRNA for binding to cytoplasmic nucleolin in these breast cancer cell lines. This interferes with the stabilization of *bcl-2* mRNA by nucleolin and may be one mechanism by which AS1411 induces tumor cell death. [Cancer Res 2008;68(7):2358–65]

Introduction

Aptamers are short DNA, RNA, or peptide oligomers that assume specific and stable three-dimensional structures in solution and in cells. The 26-mer DNA aptamer AS1411 is currently undergoing clinical evaluation in acute myeloid leukemia (AML). This guanine-rich aptamer has unmodified phosphodiester linkages and forms a G-quadruplex structure (1) that is resistant to degradation by serum enzymes (2). The stable conformation of AS1411 allows it to bind to its target protein with high affinity and specificity (3).

Although AS1411 is known to bind to nucleolin with high affinity, the biological consequences of this interaction are not well understood. Because nucleolin is a multifunctional protein that interacts with both DNA and RNA, binding of AS1411 to nucleolin could interfere with a variety of cellular activities. For example, there is evidence that nucleolin, via binding of its RNA binding and COOH-terminal domains to pre-rRNA, functions as an assembly factor by bringing together the correctly folded rRNA and other components necessary for rRNA maturation and ribosome assembly (4). This protein may also be involved in exporting ribosome components to the cytoplasm while shuttling between the cytoplasm and nucleus (5). A considerable body of evidence supports a critical role for nucleolin in mRNA stabilization. Nucleolin binds to the 3′-untranslated region (3′-UTR) of amyloid precursor protein mRNA and stabilizes this mRNA (6). It is also required for the stabilization of interleukin-2 mRNA that occurs during T-cell activation (7). More recent studies have shown that nucleolin binds to an AU-rich element (ARE) in the 3′-UTR of bcl-2 mRNA in HL-60 (8) and chronic lymphocytic leukemia cells (9) and stabilizes this mRNA by protecting it from RNase degradation.

The results of recent studies on the stabilization of *bcl-2* mRNA by nucleolin in human leukemia cells have provided insights into possible mechanisms of action and antitumor selectivity of AS1411. Nucleolin protein expression is usually higher in tumor cells than in normal or premalignant cells (9–12). The overexpression of nucleolin in tumor cells is not simply related to a higher proliferation rate of tumor cells compared with normal cells because nonproliferating chronic lymphocytic leukemia cells isolated from patients overexpressed nucleolin protein 26-fold relative to normal human $CD19^+$ B cells (9). However, a striking difference between the chronic lymphocytic leukemia cells and the normal B cells was that nucleolin was detected only in the nucleus of normal B cells but was present in the nucleus and cytoplasm of chronic lymphocytic leukemia cells. It has been proposed that AS1411 first binds to nucleolin on the external surface of tumor cells and then is internalized (13). In this regard, AS1411 may exploit the shuttling activity of nucleolin to gain intracellular access. Once inside the cell, AS1411 is thought to act as a "molecular decoy" by binding with high affinity to nucleolin and thereby interfering with its intracellular functions (13). For example, recent evidence suggests that AS1411 forms a complex with nucleolin and nuclear factor-κB essential modulator, which prevents nuclear factor-κB activation (14). Normal cells may be deficient in both AS1411 uptake and in the intracellular target of AS1411 because normal cells seem to have much lower levels of nucleolin in both plasma membrane and cytoplasm (9). These properties of AS1411 may provide the basis, at least in part, for the lack of serious toxicity reported in a phase I clinical oncology trial of AS1411 (13).

The work described herein compares the effects of AS1411 on nucleolin activity in MCF-7 breast cancer cells, MDA-MB-231 breast cancer cells, and MCF-10A normal mammary epithelial cells. Specifically, our goal was to identify the biochemical mechanisms

Note: Supplementary data for this article are available at Cancer Research Online (http://cancerres.aacrjournals.org/).

Requests for reprints: Daniel J. Fernandes, Department of Biochemistry and Molecular Biology, Medical University of South Carolina, 176 Ashley Avenue, Charleston, SC 29425. Phone: 843-792-1449; Fax: 843-792-3200; E-mail: fernand@musc.edu.

doi:10.1158/0008-5472.CAN-07-5723

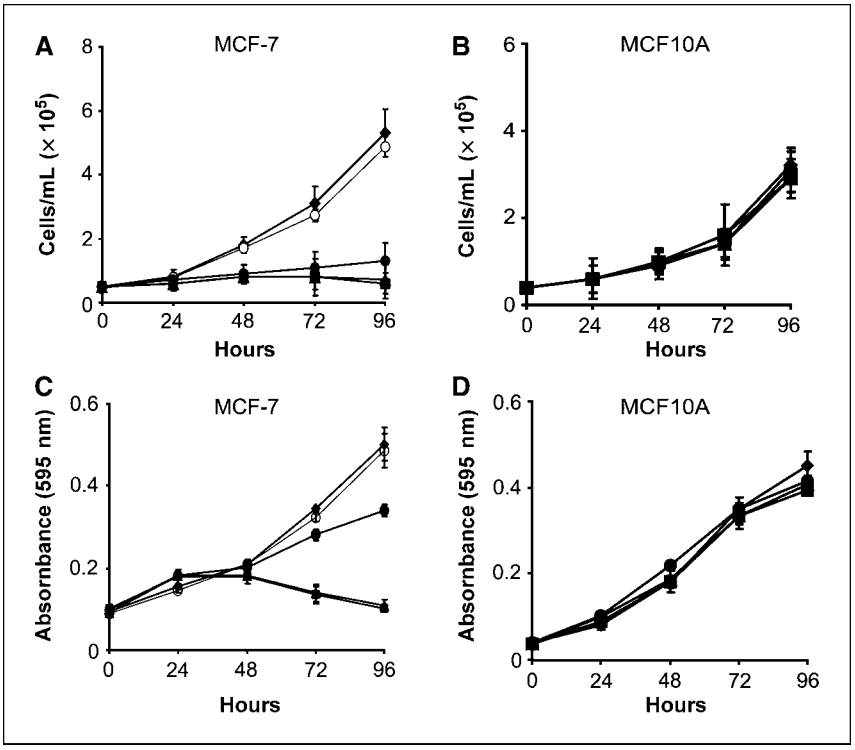

Figure 1. Inhibition of cell growth and mitochondrial activity by AS1411. MCF-7 and MCF-10A cells were incubated with AS1411 at 0 (♦), 5 (●), 10 (▲), or 20 μmol/L (■), or with CRO26 at 20 μmol/L (○), for 96 h. *A* and *C,* cell growth was measured by counting cells with a Coulter counter. *B* and *D,* mitochondrial activity was monitored by MTT assay. *Points,* mean of three (*A*) or six (*B*) experiments; *bars,* SE.

involved in the selective induction of apoptosis by AS1411 in these breast cancer cell lines relative to the normal MCF-10A cells.

Materials and Methods

Cell culture. All cultures were grown in a humidified incubator maintained at 37°C with 95% air/5% CO_2. MCF-10A normal human mammary epithelial cells were obtained from the American Type Culture Collection and were propagated in MEGM complete growth medium supplemented with bovine pituitary extract (Cambrex Bioscience). MCF-7 and MDA-MB-231 human breast cancer cells were grown in RPMI 1640 and DMEM, respectively, supplemented with 10% heat-inactivated fetal bovine serum, 0.1 mg/mL streptomycin, and 100 units/mL penicillin. Cell counting and measurements of cell viability were carried out as described (15). The numbers of apoptotic cells were determined by counting the FITC-labeled Annexin V–positive cells in a flow cytometer. AS1411, with sequence 5′-d(GGTGGTGGTGGTTGTGGTGGTGGTGG)-3′, and 5′-FITC-AS1411 were obtained from (Antisoma Research, Ltd.). AS1411 was dissolved in tissue culture media before addition to cell cultures and was dissolved in water for the cell-free experiments.

Immunoblot analysis. Immunoblotting was done as previously described (15). For determination of cytosolic nucleolin and total cellular bcl-2 proteins, cells were lysed for 15 min on ice in lysis buffer (15), followed by centrifugation at 10,000 × *g* for 15 min at 4°C. The S10 supernatant is referred to as the S10 cytosolic extract and the pellet is termed the S10 nuclear pellet. Protein concentrations were determined by the bicinchoninic acid assay (Pierce). Aliquots of the S10 cytosolic extracts containing 25 μg of protein were electrophoresed on a 12% polyacrylamide SDS gel and transblotted. Antihuman bcl-2 monoclonal antibody (mAb; clone Bcl-2 100), antihuman nucleolin mAb (clone MS-3), and antigoat actin polyclonal antibody (I-19) were purchased from Santa Cruz Biotechnology, Inc. The amounts of each protein in the blots were determined by counting the total numbers of pixels in each band (integrated density value) with ChemiImager digital imaging system (Alpha Innnotech) and/or Typhoon PhosphorImager (GE Healthcare). Values that were within the linear range of the assay were normalized to either β-actin for the cytosolic extracts or histone 2B for the nuclear extracts.

Confocal microscopy. Cells were grown on MatTek plates (MatTek Corp.). To stain plasma membrane and cytoplasmic nucleolin, the cells were fixed for 20 min at room temperature in PBS (140 mmol/L NaCl, 2.7 mmol/L KCl, 10 mmol/L Na_2HPO_4, 1.8 mmol/L KH_2PO_4, pH 7.4) containing 4% paraformaldehyde. Nonspecific binding of antibody was blocked with 3% bovine serum albumin (BSA) and 1% goat serum in PBS (blocking buffer) for 1 h at room temperature. The cells were incubated overnight at 4°C with primary anti-nucleolin antibody (Santa Cruz Biotechnology, clone MS-3; 1:100 dilution in blocking buffer), washed thrice in PBS, and incubated with secondary FITC-conjugated goat anti-mouse IgG (diluted 1:100 in blocking buffer) for 1 h at room temperature. RNA in the fixed cells was digested with RNase A (100 μg/mL for 15 min at room temperature) and propidium iodide (4 μg/mL) was used to stain DNA. The cells were washed thrice in PBS and then observed under a Carl Zeiss LSM5 Pascal confocal microscope. Confocal images (1,024 × 768 pixels) were obtained using a 63× objective lens and the images were overlaid using Carl Zeiss LSM Pascal image browser 4.0 software. Confocal images of 5′-FITC-AS1411 were also carried out using this procedure.

Measurement of *Bcl-2* mRNA stability. MCF-7, MDA-MB-231, or MCF-10A cells were incubated with no drug, 10 μmol/L AS1411, or 20 μmol/L CRO26 for 72 h. The cells were then incubated with either 0.5% ethanol or 3 μg/mL actinomycin D in 0.5% ethanol. Aliquots were removed from the cultures at times 0, 2, 4, and 8 h. Actinomycin D at this concentration did not induce any DNA fragmentation during this time period. At the various time points, 2×10^7 cells were harvested by centrifugation and washed with PBS. Total RNA was isolated using TriZol (Invitrogen), and the RNA concentrations were determined spectrophotometrically at 260 nm. Equal amounts of total RNA (2–5 μg) from each sample were reverse transcribed using Moloney murine leukemia virus (MMLV) reverse transcriptase and random hexamers. PCR amplification of the cDNAs was carried out with primer pairs for the *bcl-2* message (5′-GGAAGTGAACATTTCGGTGAC-3′; 5′-GCCTCTCCTCACGTTCCC-3′) and the *β-actin* message (5′-GCGGGAAATCGTGCGTGACAT-3′; 5′-GATGGAGTTGAAGGTA-GTTC-3′). All PCR primers were obtained from Integrated DNA Technologies, Inc. The reaction mixture contained 200 nmol/L dATP, dCTP, dGTP, and dTTP; primers at 200 nmol/L each; 2.5 units of HotStart Taq DNA polymerase (Qiagen), which lacks 3′-5′ exonuclease activity; 2.5 mmol/L $MgCl_2$; and 1 μL

of cDNA product in a final volume of 25 μL. The HotStart Taq DNA polymerase was activated by a 15-min incubation at 95°C in the thermal cycler. This was followed by template denaturation for 1 min at 94°C, primer-template annealing for 1 min at 57°C, and then primer extension for 1 min at 72°C. After 26 cycles for bcl-2 and 24 cycles for β-actin, the extension reactions were continued for an additional 7 min at 72°C. The PCR products were separated on a 1% agarose gel and stained with ethidium bromide, and product formation was quantitated by determining the integrated density value of each band. Product formation was linear over the range of the amounts of cDNA and PCR cycles used.

Coimmunoprecipitation of nucleolin-Bcl-2 mRNA complexes. Immunoprecipitation of nucleolin-*bcl-2* mRNA complexes was done as previously described (8) with the following modifications. Briefly, cells were harvested by centrifugation at 100 × *g* for 5 min at 4°C and then suspended in 10 mL of PBS. Formaldehyde was added to the cell suspension to a final concentration of 1.0% (v/v) and the reaction was incubated at room temperature for 10 min with slow mixing. Cross-linking was quenched by the addition of glycine (pH 7.0, 0.125 mol/L final concentration), followed by incubation of the mixture at room temperature for 5 min. The cells were washed thrice with 10 mL of PBS and once with 1.0 mL of RIPA buffer (16). The pellet was resuspended in 0.5-mL RIPA buffer and sonicated for three rounds of 20 s each at output level 7 of a Misonix 300 sonicator (Fisher Scientific). The sonicated samples were cleared by centrifugation for 10 min at 17,000 × *g*, and the supernatants were split into two 0.25-mL aliquots and used immediately for immunoprecipitation. One aliquot was saved as the input sample and the other aliquot was mixed with 20 μL of Protein A-Sepharose beads (Santa Cruz Biotechnology) for 1 h at 4°C followed by centrifugation at 400 × *g* for 5 min. The precleared supernatant was diluted with 250-μL RIPA buffer containing RNasin and protease inhibitors, mixed with either anti-nucleolin (3 μg/mL) or IgG mAb (3 μg/mL), and incubated overnight with shaking at 4°C. Protein A-Sepharose beads were added and the samples were incubated with shaking for 3 h at 4°C. The Sepharose beads were washed five times with high stringency buffer (16) and then incubated at 70°C for 45 min to reverse cross-linking. RNA was extracted from the input and the immunoprecipitated samples using TriZol and then treated with DNase I. The RNA was used to synthesize cDNA using random hexamer primers and MMLV reverse transcriptase as described above. Reverse transcription reactions were carried out for 1 h at 42°C. Real-time quantitative PCR was done using 2 μL of the cDNA sample for 40 cycles of amplification. The PCR primers for *bcl-2* ARE-1 mRNA were 5′-CAGTCTT-CAGGCAAAACGTCGA-3′ and 3′-TGGTCGGATTTCCAAAGACA-5′. Amplification of 18S rRNA was carried out using the Quantum RNA Universal 18S Kit from Ambion, Inc., and served as an internal control for data normalization. The fold enrichment of *bcl-2* mRNA sequences in the immunoprecipitates relative to the nonprecipitated imput samples was calculated using the standard $\Delta\Delta C_t$ method (Stratagene *Introduction to Quantitative PCR* manual IN #70200-00).

RNA gel mobility shift assay. This assay was done as previously described (17). Recombinant nucleolin was generated using a bacterial expression vector (pET21a) containing cDNA sequences that code for residues 284 to 707 of human nucleolin [Δ1–283 Nuc-$(His)_6$; refs. 8, 18]. Briefly, 50 nmol/L of recombinant nucleolin, a 29-nucleotide (nt) *bcl-2* ARE-1 RNA sequence (50 nmol/L, 20,000 cpm), and 0, 12.5, 25, 37.5, 50, and 100 nmol/L concentrations of competitor AS1411 were incubated on ice for 10 min in 20 μL of RNA binding buffer [50 mmol/L Tris-HCl (pH 7.5), 150 mmol/L NaCl, 0.025 mg/mL tRNA, 0.25 mg/mL BSA]. Five microliters of gel loading solution (50% glycerol, 0.1% bromophenol blue, 0.1% xylene-cyanol) were then added to the reaction, and 10 μL of each reaction mixture were analyzed on a 6% PAGE/Tris-borate EDTA gel, which was dried on nitrocellulose paper and analyzed by phosphorimaging with Typhoon PhosphorImager.

Generation of nucleolin siRNA transfectants. Nucleolin was knocked down in MCF-7 cells by transfecting the cells with a plasmid containing a

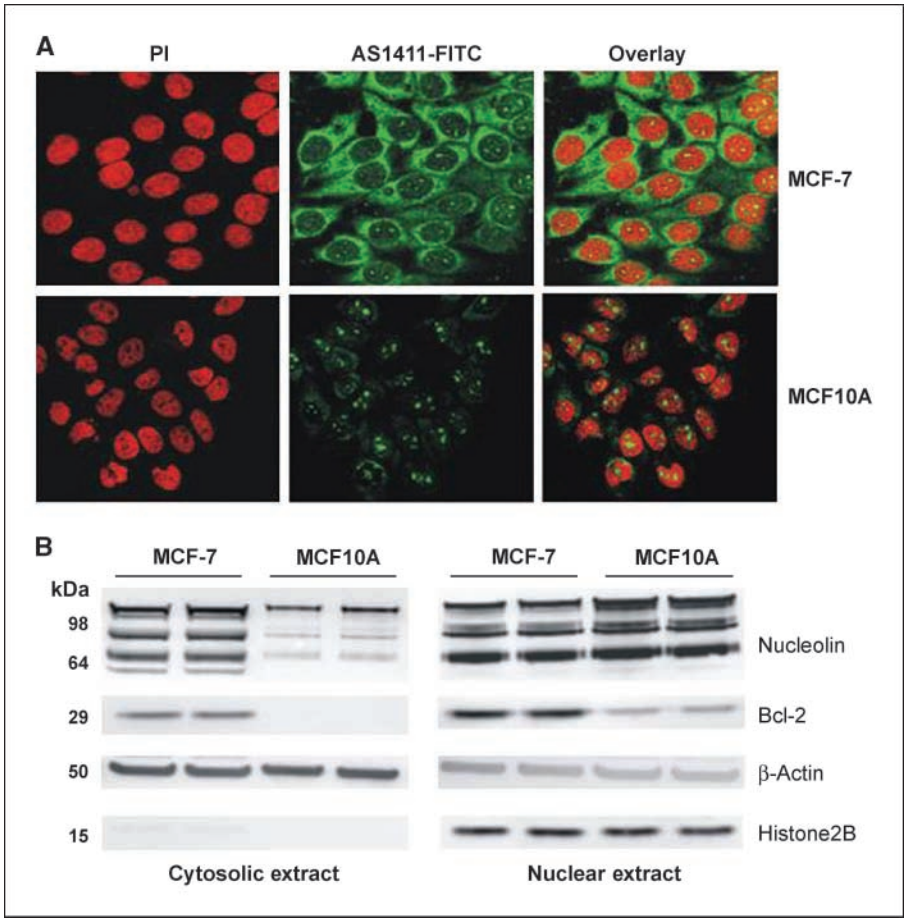

Figure 2. *A,* cellular uptake of AS1411 in MCF-7 and MCF-10A cells. The binding of AS1411 was determined by confocal imaging of immunofluorescence of FITC labeled AS1411. Nuclei were counterstained with propidium iodide (*PI*). Representative images of three separate experiments. *B,* levels of nucleolin and bcl-2 protein in MCF-7 and MCF-10A cells. The levels of nucleolin and bcl-2 protein were determined by immunoblotting with mAbs specific for nucleolin and bcl-2 proteins. The relative amounts of protein were calculated after normalization to β-actin for the cytosolic extracts and to histone 2B for nuclear extracts.

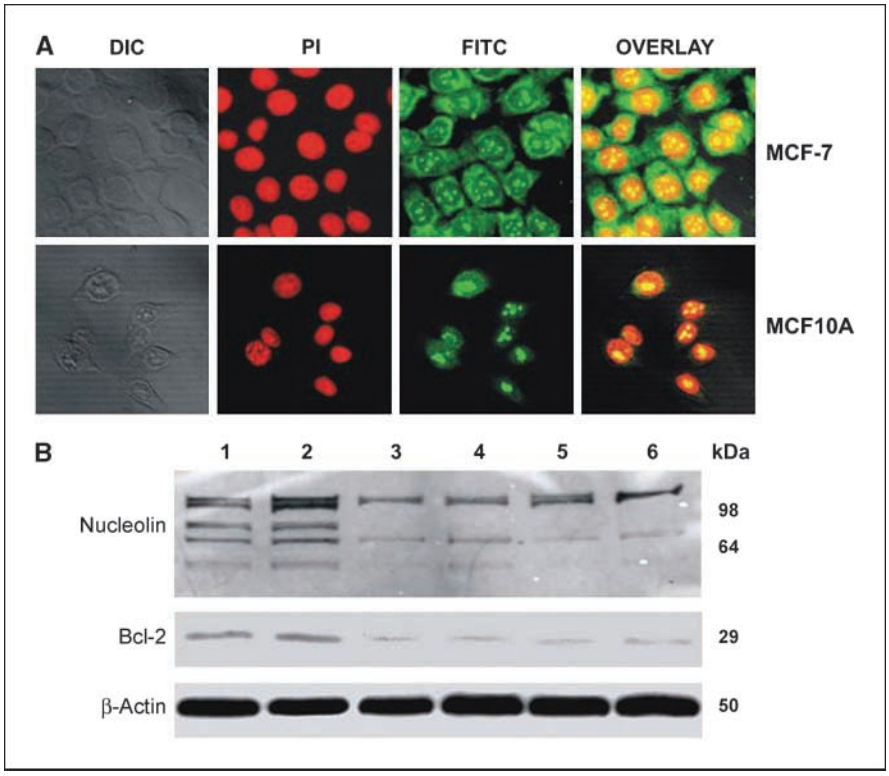

Figure 3. *A,* subcellular localization of nucleolin in MCF-7 and MCF-10A cells. The intracellular localization of nucleolin was determined by indirect immunofluorescence with a mAb against human nucleolin and a secondary FITC-conjugated antimouse IgG. Nuclei were counterstained with propidium iodide. Cell morphology is shown as differential interference contrast images. Representative results of three separate experiments. *B,* siRNA knockdown of nucleolin in stable clones of MCF-7 cells. The cells were transfected with either a scrambled siRNA (*lanes 1* and *2*) or a nucleolin siRNA (*lanes 3–6*). S10 cell extracts were prepared and the amounts of immunoreactive nucleolin, bcl-2, and β-actin proteins were determined by Western blotting.

nucleolin siRNA (hNuc) as previously described (9). MCF-7 cells were also transfected with a plasmid expressing a scrambled siRNA with limited homology to any known human genomic sequence. The nucleolin and scrambled siRNA sequences in the G418-resistant clones were confirmed by sequencing.

Total RNA was extracted from the transfectants using TriZol reagent. Nucleolin and *bcl-2* mRNA levels were analyzed by quantitative PCR in the stable clones. cDNA synthesis was done using 2 μg of total RNA as described above. The primers for nucleolin and *bcl-2* were 5′-CCAGCCATC-CAAAACTCTGT-3′ and 5′-TAACTATCCT-TGCCCGAACG-3′ and 5′-ATGTGTGTGGAGAGCGTCAA-3′ and 5′-ACAGTTCCACAAAGGCATCC-3′, respectively. The primers for β-*actin* were 5′-AAATCTGGCACCA-CACCTTC-3′ and 5′-GGGGTGTTGAAGGTCTCAAA-3′. All primers were purchased from Integrated DNA Technologies, Inc. cDNA was amplified using a Brilliant SYBR Green QPCR Master Mix from Stratagene. The reaction was carried out at 95°C for 10 min, followed by 40 cycles of 95°C for 30 s, 53°C for 90 s, and 72°C for 60 s. Nucleolin and *bcl-2* mRNAs were quantified and normalized relative to β-actin mRNA. Each reaction was done in duplicate and the comparative C_t method was used for relative quantification of gene expression.

Results

Effect of AS1411 on the growth and viability of human MCF-7, MDA-MB-231, and MCF-10A cells. Initial studies were done to compare the relative sensitivities of MCF-7 and MDA-MB-231 breast cancer cells and MCF-10A normal breast epithelial cells to AS1411. AS1411 at 5 μmol/L completely inhibited the proliferation of MCF-7 cells but loss of mitochondrial activity was not observed until 72 hours after drug exposure (Fig. 1*A* and *C*). However, 20 μmol/L CRO26 [5′-d(CCTCCTCCTCCTTCTCCTCCT-CCTCC)-3′], a 26-mer cytosine-rich control oligonucleotide that does not form a stabilized quadruplex structure (1, 2), had no effect on either MCF-7 cell growth (Fig. 1*A*) or mitochondrial activity (Fig. 1*C*). Consistent with the results of the 3-(4,5-dimethylthiazol-2-yl)-2,5-diphenyltetrazolium bromide (MTT) assay, the AS1411-treated cells became apoptotic by 72 hours. At 72 hours, 5 ± 0.1%, 44 ± 16%, and 59 ± 3% of the MCF-7 cells incubated with 0, 5, or 10 μmol/L AS1411, respectively, were Annexin V positive. These data indicate that AS1411 first induces a cytostatic effect in MCF-7 cells, which is then followed by cell death. AS1411 had similar effects on the growth rate and mitochondrial activity of MDA-MB-231 breast cancer cells (Supplementary Fig. S1). In contrast to that observed with the breast cancer cell lines, 20 μmol/L AS1411 had no effect on the growth rate (Fig. 1*B*), mitochondrial activity (Fig. 1*D*), or viability (data not shown) of normal MCF-10A cells following exposure times as long as 96 hours.

The greater sensitivity of MCF-7 breast cancer cells to AS1411 compared with normal MCF-10A cells was related to the more extensive uptake of AS1411 into MCF-7 cells (Fig. 2*A*). The intracellular localization of AS1411 was determined by confocal imaging of FITC-conjugated AS1411 fluorescence after a 1-hour incubation of the cells with 2 μmol/L drug. The cells were incubated with propidium iodide to counterstain the nuclei (red fluorescence). Figure 2*A* shows that the accumulation of AS1411 was much greater in the cytoplasm of MCF-7 cells than in MCF-10A cells. Both cell lines showed a punctate distribution of AS1411 in the nucleus.

Expression and localization of nucleolin in MCF-7, MDA-MB-231, and MCF-10A cells. AS1411 has been shown to bind tightly to nucleolin in some tumor cells (3). Thus, we determined the relative amounts and intracellular localization of nucleolin in MCF-7 and MCF-10A cells to determine whether differences in either the expression levels or localization of nucleolin in these cell lines were related to the greater sensitivity of MCF-7 cells to AS1411. We compared the relative levels of nucleolin and bcl-2 proteins in MCF-7 and MCF-10A cells by immunoblotting S10 supernatants of these cells. We chose to analyze S10 supernatants to permit measurement of nonnuclear nucleolin, which we

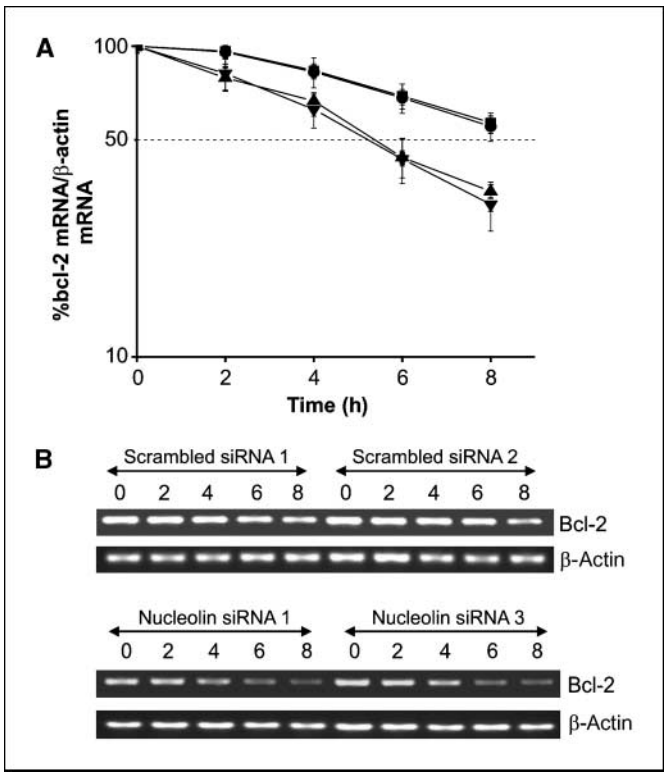

Figure 4. Effect of nucleolin knockdown on the half-life of *bcl-2* mRNA in MCF-7 cells. *A,* levels of total intracellular *bcl-2* mRNA were measured by reverse transcription-PCR (RT-PCR) in two clones of scrambled siRNA–transfected cells (■, ●) and two clones of cells transfected with a nucleolin siRNA (▲, ▼). Semiquantitative RT-PCR was used to analyze bcl-2 mRNA levels at the indicated time points (0, 2, 4, 6, and 8 h) after the addition of actinomycin D. Data were normalized to β-actin mRNA and plotted on a semilogarithmic scale. *Points,* mean of three experiments; *bars,* SE. *B,* the PCR products were analyzed on a 2% agarose gel, which was stained with ethidium bromide and analyzed with ChemiImager digital imaging system.

postulate is directly involved in *bcl-2* mRNA stabilization, and mitochondrial bcl-2 protein in the same cell extract. This analysis revealed that full-length nucleolin protein (106 kDa) and its degradation products (19) were 4-fold elevated ($P < 0.007$) in S10 cytoplasmic extracts of MCF-7 cells compared with MCF-10A cells (Fig. 2*B*). No statistically significant differences in the nuclear (S10 pellet) levels of nucleolin were observed between MCF-7 and MCF-10A cells ($P > 0.05$). Immunoblotting also revealed high levels of cytosolic nucleolin in S10 extracts of MDA-MB-231 breast cancer cells (Supplementary Fig. S2) compared with MCF-10A cells (Fig. 2*B*). The nuclear protein histone 2B was not detected in the blots of the S10 extracts from MCF-7, MDA-MB-231, or normal MCF-10A cells. Thus, the presence of high levels of nucleolin in the S10 cytoplasmic extracts of MCF-7 and MDA-MB-231 cells was not consistent with the contamination of the S10 extracts with nuclear nucleolin. Bcl-2 protein was detected in both the cytosolic and nuclear fractions from MCF-7 and MDA-MB-231 cells but was undetectable in the S10 cytosol from MCF-10A cells.

Results from confocal microscopy studies on the localization of nucleolin (Fig. 3*A* and Supplementary Fig. S2) were consistent with the immunoblotting data. The intracellular localization of nucleolin was determined by indirect immunofluorescence with primary antibody against nucleolin and a FITC-conjugated antimouse IgG secondary antibody (green fluorescence). The DNA was stained with propidium iodide (red fluorescence). The overlay images in Fig. 3*A* and Supplementary Fig. S2 indicate that nucleolin was present throughout the nucleus (yellow fluorescence) and cytoplasm (green fluorescence) of MCF-7 cells and MDA-MB-231 cells, whereas in MCF-10 cells nucleolin was detected only in the nucleus. When taken together, the results in Figs. 1–3*A* indicate that MCF-7 breast cancer cells show greater uptake of AS1411 into the cytoplasm, higher cytoplasmic levels of nucleolin, and much greater sensitivity to AS1411 than normal MCF-10A cells.

AS1411 inhibits the stabilization of Bcl-2 mRNA by nucleolin in MCF-7 and MDA-MB-231 cells. Our previous studies with HL-60 leukemia cells (8) and chronic lymphocytic leukemia cells from patients (9) showed that nucleolin binds to an ARE instability

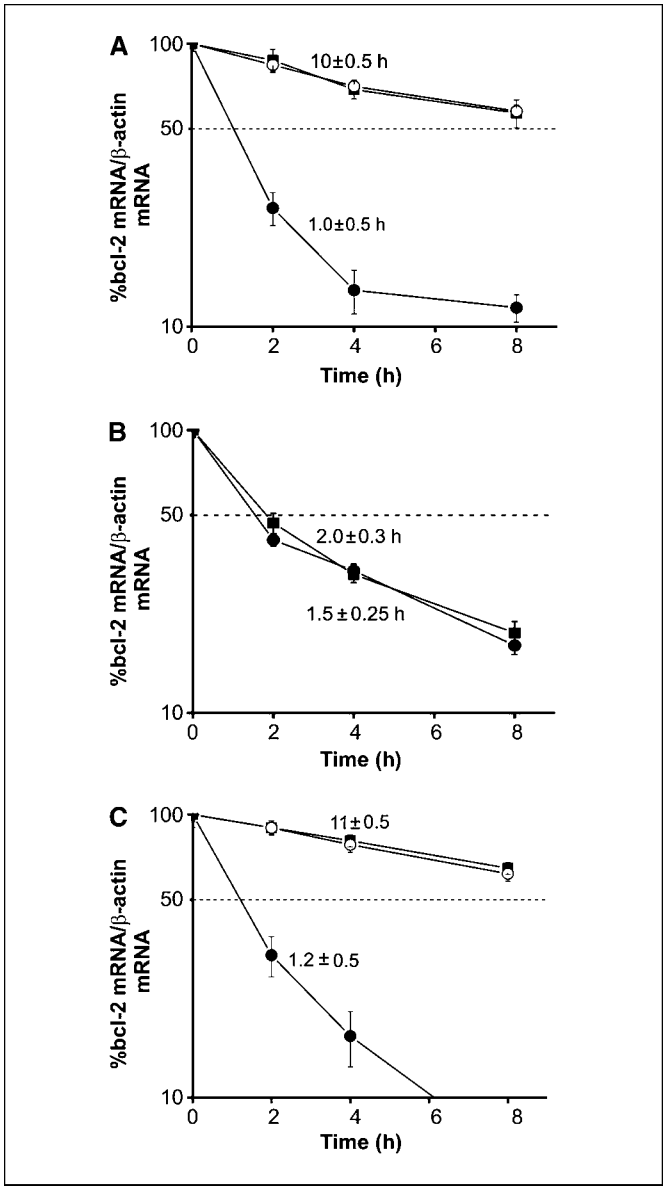

Figure 5. Effect of AS1411 on the half-life of *bcl-2* mRNA in MCF-7, MDA-MB-231, and MCF-10A cells. Levels of total intracellular *bcl-2* mRNA were measured by RT-PCR in control cells (■) and cells treated with 10 μmol/L AS1411 (●). Cells were incubated with 10 μmol/L AS1411 for 72 h and semiquantitative RT-PCR was used to analyze bcl-2 mRNA levels at the indicated time points (0, 2, 4, and 8 h) after the addition of actinomycin D. Data were normalized to β-actin mRNA. *Points,* mean of three experiments; *bars,* SE. *A,* MCF-7 cells. *B,* MCF-10A cells. *C,* MDA-MB-231 cells.

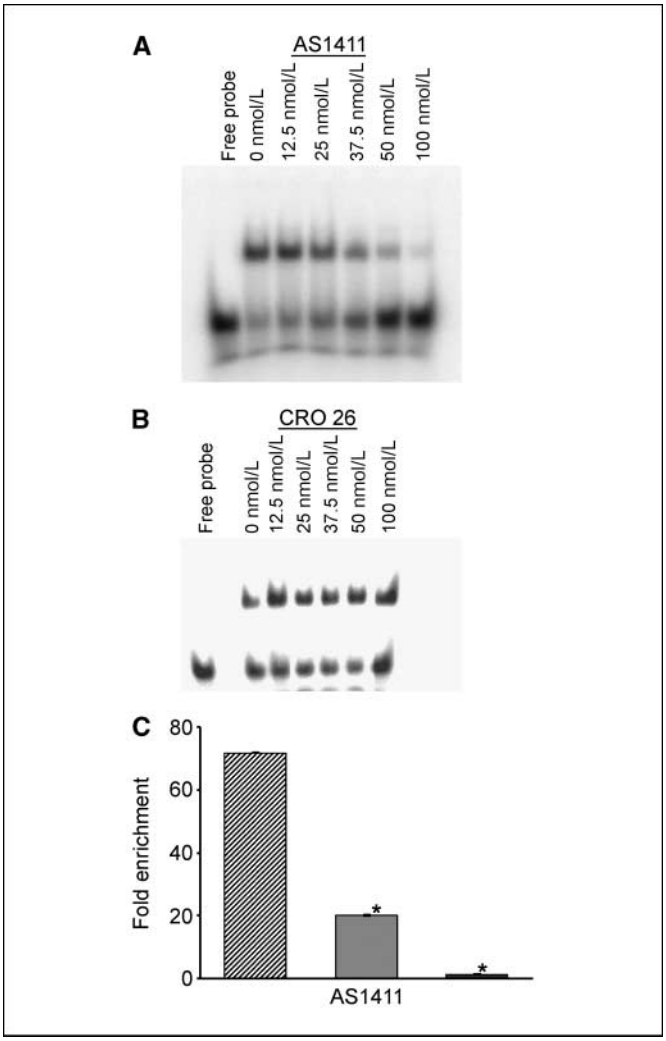

Figure 6. *A,* competition gel shift assay of AS1411 and a 29-nt ARE element in *bcl-2* mRNA for binding to recombinant nucleolin. ^{32}P-RNA (50 nmol/L) was incubated with 50 nmol/L nucleolin in the presence of increasing concentrations of unlabeled AS1411 aptamer. *Lane 1,* free probe; *lanes 2* to *7,* 0, 12.5, 25, 37.5, 50, and 100 nmol/L AS1411, respectively. Complexes were analyzed on a native 6% polyacrylamide gel and detected by phosphorimaging. *B,* competition gel shift assay of a 26-nt CRO26 and a 29-nt ARE element in *bcl-2* mRNA for binding to recombinant nucleolin. The assay was carried out as described in Fig. 5*A*. *C,* effect of AS1411 on the binding of nucleolin to *bcl-2* mRNA in MCF-7 cells. The cells were cultured in the absence (▨) or presence of 5 μmol/L (▤) or 10 μmol/L (■) of AS1411 for 72 h. Cell lysates were prepared and the nucleolin-*bcl-2* mRNA complexes were immunoprecipitated with anti-nucleolin antibody. The *bcl-2* mRNA in the immunoprecipitates was analyzed by real-time quantitative PCR with *bcl-2* ARE-1 mRNA primers. *Columns,* mean of three experiments; *bars,* SE.

element in the 3′-UTR of *bcl-2* mRNA and protects this mRNA from degradation (8, 9). Experiments were done to determine whether nucleolin has a similar activity in MCF-7 and MDA-MB-231 cells and if AS1411 could interfere with the stabilization of *bcl-2* mRNA by nucleolin in these cell lines. If nucleolin is an important *trans*-acting factor required for the stabilization of *bcl-2* mRNA, then knockdown of nucleolin with a siRNA should lead to destabilization of *bcl-2* mRNA. To test this, nucleolin was knocked down partially in MCF-7 breast cancer cells by transfecting the cells with a nucleolin siRNA plasmid. Complete knockdown of nucleolin was not compatible with survival of the MCF-7 cells. Control MCF-7 cells were transfected with a plasmid expressing a scrambled siRNA with limited homology to any known human genomic sequence. Nucleolin and *bcl-2* mRNA levels were determined by real-time PCR analysis in two MCF-7 clones transfected with a scrambled siRNA and four clones transfected with the nucleolin siRNA. The levels of nucleolin mRNA and *bcl-2* mRNA in the stable nucleolin siRNA–transfected clones were reduced to 24 ± 3% SE and 17 ± 5% SE, respectively, of the corresponding levels measured in the two MCF-7 clones transfected with the scrambled siRNA. To determine if the reduction in *bcl-2* mRNA was the result of decreased mRNA stability, the half-life of *bcl-2* mRNA was measured after incubation of the clones with actinomycin D to block transcription. The half-life of *bcl-2* mRNA was 5 hours in the nucleolin siRNA–transfected clones and 11 hours in the scrambled siRNA clone (Fig. 4). Western blot analysis of the transfectants revealed that the levels of full-length nucleolin (106 kDa) and its proteolysis products (19) were down-regulated in all four clones transfected with the nucleolin siRNA compared with the two clones transfected with the scrambled siRNA (Fig. 3*B*). Equally important, nucleolin knockdown was accompanied by down-regulation of bcl-2 protein, but not β-actin, in the four clones transfected with the nucleolin siRNA. These results indicate that nucleolin down-regulation in MCF-7 cells leads to *bcl-2* mRNA instability and decreased levels of bcl-2 protein in MCF-7 cells.

Similar to the nucleolin siRNA, the nucleolin-targeting aptamer AS1411 also decreased the stability of *bcl-2* mRNA. The half-life of *bcl-2* mRNA was reduced from 10 hours in untreated MCF-7 cells to 1 hour in MCF-7 cells incubated with 10 μmol/L AS1411 for 72 hours (Fig. 5*A*). Likewise, AS1411 reduced the half-life of *bcl-2* mRNA in MDA-MB-231 cells from 11 to 1.2 hours (Fig. 5*C*). In contrast, 10 μmol/L AS1411 had no effect on the stability of *bcl-2* mRNA in normal MCF-10A cells (Fig. 5*B*).

AS1411 interferes with binding of nucleolin to *bcl-2* mRNA. Further studies examined the effect of AS1411 on the binding of *bcl-2* mRNA to either purified recombinant nucleolin or endogenous nucleolin in MCF-7 cells. As a first step in mapping of the binding site of nucleolin on *bcl-2* ARE-1, binding of recombinant nucleolin to four contiguous fragments of the ARE was examined (fragments 5′-A,B,C,D-3′). Human recombinant nucleolin [Δ1–283Nuc-$(His)_6$] was found to bind with highest affinity to fragment B, which consists of a 29-nt sequence, 5′-CCAAAGGGAAAUAUCAUUUAUUUUUUACA-3′, located 70 nt downstream from the *bcl-2* stop codon. This AU-rich sequence contains the pentamer AUUUA within the loop of a potential stem-loop structure and binds to human nucleolin [Δ1–283Nuc-$(His)_6$] in gel shift assays with high affinity [average association constant, 0.38 $(nmol/L)^{-1}$; range of two experiments, 0.31–0.48 $(nmol/L)^{-1}$]. Competition binding assays were then done with the 29-nt bcl-2 ARE sequence and either AS1411 (Fig. 6*A*) or the control C-rich oligonucleotide (CRO26; Fig. 6*B*) for binding to human recombinant nucleolin. Assays were done with a fixed amount of the 29-nt ARE sequence in the presence of increasing concentrations of AS1411 or CRO26. Fig. 6*A* reveals a dose-dependent decrease in nucleolin binding to the *bcl-2* ARE element with increasing concentrations of unlabeled AS1411. Quantitation of the data in Fig. 6*A* revealed that AS1411 at 25 and 37.5 nmol/L reduced binding of the 29-nt *bcl-2*-ARE sequence (50 nmol/L) to nucleolin to 58 ± 0.1% SE and 38 ± 0.1% SE, respectively, compared with reactions lacking AS1411. In contrast, the control oligonucleotide CRO26, which lacks antiproliferative activity (Fig. 1), had no significant effect on the binding of the *bcl-2*-ARE sequence to nucleolin (Fig. 6*B*). These results indicate that

AS1411 competes effectively with *bcl-2* ARE RNA for binding to recombinant nucleolin in a cell-free assay.

Inhibition of nucleolin binding to *bcl-2* mRNA by AS1411 in MCF-7 cells was examined by incubating the cells with 0, 5, or 10 μmol/L AS1411 for 72 hours, followed by coimmunoprecipitation of endogenous nucleolin-*bcl-2* mRNA complexes with anti-nucleolin antibody. The RNA was then reversed transcribed and real-time quantitative PCR was done using primers specific for *bcl-2* mRNA. The fold enrichment of *bcl-2* mRNA sequences in the immunoprecipitates over nonprecipitated input RNA was reduced from 72 ± 0.1 SE (control) to 20 ± 0.34 SE (72% decrease) and 1 ± 0.1 SE (99% decrease) in cells incubated with 5 and 10 μmol/L AS1411, respectively (Fig. 6*C*). Thus, AS1411, at a minimally cytotoxic concentration (5 μmol/L, Fig. 1), was able to inhibit binding of nucleolin to *bcl-2* mRNA in MCF-7 cells. In summary, Fig. 6*A* and *C* suggests that AS1411 acts as a molecular decoy in MCF-7 cells by competing with *bcl-2* RNA for binding to nucleolin.

Discussion

AS1411 represents a new paradigm for cancer therapy because it is the first aptamer to be evaluated in human oncology trials and seems to be the first anticancer agent shown to induce mRNA instability. It has shown both promising antitumor activity and a lack of serious systemic toxicity in a phase I trial (13). A program of phase II studies, including trials in AML, is now under way.

The nucleic acid binding protein nucleolin is thought to be an important cellular target for AS1411. Nucleolin has been shown to bind to G-quadruplex–forming DNA sequences (3, 20). Thus, the stable G-quadruplex structure of AS1411 may promote high affinity and specific binding of the aptamer to nucleolin. In this regard, AS1411 may function as a chemical antibody' (21). The results reported herein are supportive of this concept. Figure 6*A* and *C* shows that AS1411 was a potent inhibitor of nucleolin binding to bcl-2 mRNA in a cell-free system and in MCF-7 cells.

Based on the data presenter herein, a molecular decoy model of AS1411 action is proposed to explain the much greater toxicity of AS1411 to tumor cells compared with normal cells. According to this model, the high antitumor selectivity of AS1411 is the result of overexpression of nucleolin in the cytoplasm and possibly the plasma membrane of tumor cells compared with normal cells. Immunoblotting and confocal microscopy showed that nucleolin was overexpressed in $CD19^+$ chronic lymphocytic leukemia cells from patients relative to $CD19^+$ B cells from healthy human volunteers (9). Previous studies showed that cytoplasmic nucleolin binds to the ARE-1 instability element in the 3′-UTR of *bcl-2* mRNA and protects this mRNA from degradation (8). Nucleolin is an important protein involved in *bcl-2* mRNA stabilization because siRNA knockdown of nucleolin is sufficient to induce *bcl-2* mRNA destabilization and down-regulation (Fig. 3*B*). In addition, recombinant nucleolin alone, when added to S100 extracts of normal $CD19^+$ B cells, slowed the rate of *bcl-2* mRNA decay to that observed in chronic lymphocytic leukemia cells (9). Thus, in MCF-7 and chronic lymphocytic leukemia cells, *bcl-2* mRNA is abnormally stabilized, which allows the tumor cells to overproduce bcl-2 protein and avoid apoptosis.

It follows from this model that AS1411, by acting as a molecular decoy, competes with *bcl-2* ARE mRNA for binding to nucleolin and thereby induces *bcl-2* mRNA instability and apoptosis. This will occur to a much greater extent in tumor cells such as MCF-7 cells and chronic lymphocytic leukemia cells than in normal cells because normal cells do not overexpress nucleolin in the cytoplasm and do not depend on stabilization of *bcl-2* mRNA for survival. Antitumor selectivity may be obtained at an additional level. It has been proposed that AS1411 binds to nucleolin that is present on the external surface of tumor, but not normal, cells and gains intracellular access when nucleolin is shuttled from the plasma membrane to the cytoplasm and nucleus (13). This hypothesis is consistent with our observation that AS1411 accumulated to a much greater extent in the cytoplasm of MCF-7 cells compared with MCF-10A cells. Our confocal microscopy images are also consistent with the presence of nucleolin on the cell surface of MCF-7 and chronic lymphocytic leukemia cells, but not on normal mammary epithelial cells or normal $CD19^+$ B cells (9). Nevertheless, further studies are required on the putative role of nucleolin as a cell-surface receptor for AS1411 in tumor cells.

Because nucleolin is a multifunctional protein, it is possible that binding of AS1411 to nucleolin interferes with multiple biological activities in tumor cells. Inhibition of DNA synthesis is observed in tumor cells that are sensitive to G-rich DNA aptamers (22). This may be related to formation of complexes of the aptamers with nucleolin and nuclear factor-κB essential modulator, which prevents nuclear factor-κB activation and cell growth signaling (14). However, inhibition of DNA synthesis by AS1411 is likely not the only mode of action of this aptamer. We have found that AS1411 induces apoptosis in indolent chronic lymphocytic leukemia cells that are not replicating DNA, as evidenced by the negligible rate of [^{3}H]thymidine incorporation into DNA in these cells.[3] The ability of AS1411 to induce apoptosis in indolent tumor cells via down-regulation of bcl-2 protein[3] suggests that this aptamer may show activity against some solid tumors that have a low growth fraction. The strong mechanistic rationale for the antitumor effects of a nucleolin targeting aptamer combined with predictive preclinical pharmacology and promising phase I clinical results underpins further investigation of AS1411 in cancer clinical trials.

[3] Unpublished observations.

Acknowledgments

Received 10/2/2007; revised 1/23/2008; accepted 1/29/2008.

Grant support: National Cancer Institute grant CA109254 and an unrestricted research grant from Antisoma, Ltd., London, United Kingdom.

The costs of publication of this article were defrayed in part by the payment of page charges. This article must therefore be hereby marked *advertisement* in accordance with 18 U.S.C. Section 1734 solely to indicate this fact.

We thank H. James Nicholson from the Department of Pathology and Laboratory Medicine at the Medical University of South Carolina for his technical assistance with confocal microscopy.

References

1. Dapic V, Abdomerovic V, Marrington R, et al. Biophysical and biological properties of quadruplex oligodeoxyribonucleotides. Nucleic Acids Res 2003;31:2097–107.

2. Dapic V, Bates PJ, Trent JO, Rodger A, Thomas SD, Miller DM. Antiproliferative activity of G-quartet-forming oligonucleotides with backbone and sugar modifications. Biochemistry 2002;41:3676–85.

3. Bates PJ, Kahlon JB, Thomas SD, Trent JO, Miller DM. Antiproliferative activity of G-rich oligonucleotides

correlates with protein binding. J Biol Chem 1999;274:26369–77.
4. Ginisty H, Sicard H, Roger B, Bouvet P. Structure and functions of nucleolin. J Cell Sci 1999;112:761–72.
5. Srivastava M, Pollard HB. Molecular dissection of nucleolin's role in growth and cell proliferation: new insights. FASEB J 1999;13:1911–22.
6. Malter JS. Regulation of mRNA stability in the nervous system and beyond. J Neurosci Res 2001;66:311–6.
7. Chen CY, Gherzi R, Andersen JS, et al. Nucleolin and YB-1 are required for JNK-mediated interleukin-2 mRNA stabilization during T-cell activation. Genes Dev 2000;14:1236–48.
8. Sengupta TK, Bandyopadhyay S, Fernandes DJ, Spicer EK. Identification of nucleolin as an AU-rich element binding protein involved in bcl-2 mRNA stabilization. J Biol Chem 2004;279:10855–63.
9. Otake Y, Soundararajan S, Sengupta TK, et al. Overexpression of nucleolin in chronic lymphocytic leukemia cells induces stabilization of bcl2 mRNA. Blood 2007;109:3069–75.
10. Derenzini M, Sirri V, Trere D, Ochs RL. The quantity of nucleolar proteins nucleolin and protein B23 is related to cell doubling time in human cancer cells. Lab Invest 1995;73:497–502.
11. Trere D, Derenzini M, Sirri V, et al. Qualitative and quantitative analysis of AgNOR proteins in chemically induced rat liver carcinogenesis. Hepatology 1996;24:1269–73.
12. Pich A, Chiusa L, Margaria E. Prognostic relevance of AgNORs in tumor pathology. Micron 2000;31:133–41.
13. Ireson CR, Kelland LR. Discovery and development of anticancer aptamers. Mol Cancer Ther 2006;5:2957–62.
14. Girvan AC, Teng Y, Casson LK, et al. AGRO100 inhibits activation of nuclear factor-κB (NF-κB) by forming a complex with NF-κB essential modulator (NEMO) and nucleolin. Mol Cancer Ther 2006;5:1790–9.
15. Otake Y, Sengupta TK, Bandyopadhyay S, Spicer EK, Fernandes DJ. Retinoid-induced apoptosis in HL-60 cells is associated with nucleolin down-regulation and destabilization of Bcl-2 mRNA. Mol Pharmacol 2005;67:319–26.
16. Niranjanakumari S, Lasda E, Brazas R, Garcia-Blanco MA. Reversible cross-linking combined with immunoprecipitation to study RNA-protein interactions *in vivo*. Methods 2002;26:182–90.
17. Bandyopadhyay S, Sengupta TK, Fernandes DJ, Spicer EK. Taxol- and okadaic acid-induced destabilization of bcl-2 mRNA is associated with decreased binding of proteins to a bcl-2 instability element. Biochem Pharmacol 2003;66:1151–62.
18. Yang C, Maiguel DA, Carrier F. Identification of nucleolin and nucleophosmin as genotoxic stress-responsive RNA-binding proteins. Nucleic Acids Res 2002;30:2251–60.
19. Chen CM, Chiang SY, Yeh NH. Increased stability of nucleolin in proliferating cells by inhibition of its self-cleaving activity. J Biol Chem 1991;266:7754–8.
20. Hanakahi LA, Sun H, Maizels N. High affinity interactions of nucleolin with G-G-paired rDNA. J Biol Chem 1999;274:15908–12.
21. Nimjee SM, Rusconi CP, Sullenger BA. Aptamers: an emerging class of therapeutics. Annu Rev Med 2005;56:555–83.
22. Xu X, Hamhouyia F, Thomas SD, et al. Inhibition of DNA replication and induction of S phase cell cycle arrest by G-rich oligonucleotides. J Biol Chem 2001;276:43221–30.